

1 Stock assessment of the flying jumbo squid in
2 Ecuadorian waters with generalised depletion models:
3 a proof of concept note

4 Rubén H. Roa-Ureta

5 Independent consultant, Bilbao, Spain

6 ruben.roa.ureta@mail.com

7 Manuel Peralta

8 Coordinador Unidad Recursos Pelágicos, Instituto Público de

9 Investigación de Acuicultura y Pesca, Guayaquil, Ecuador

10 mperalta@institutopesca.gob.ec

11 José L. Pacheco

12 Investigador Pesquero, Unidad Recursos Pelágicos, Instituto Público de

13 Investigación de Acuicultura y Pesca

14 jpacheco@institutopesca.gob.ec

15
16 August 25, 2021

17 **Abstract**

18 The flying jumbo squid fishery is one of the largest fisheries of the world and
19 the largest invertebrate fishery. In the region of the South-East Pacific Ocean
20 (SEP) it is fished in four sub-regions: Ecuadorian, Peruvian and Chilean exclusive
21 economic zones (EEZ), and international waters off those EEZs. In this meeting
22 of OROP-PS, the CALAMASUR group is proposing a regional stock assessment
23 model that includes flows among these sub-regions (Wiff and Roa-Ureta, 2021).
24 Therefore the question arises: is there any evidence for flows of the stock among
25 sub-regions? In this note I explored this issue by modelling Ecuadorian catch, effort
26 and mean weight data taken during 2018 using intra-annual generalized depletion
27 models (Roa-Ureta, 2012). The model runs on weekly time steps and the presence
28 of pulses of abundance that enter the Ecuadorian sub-region is tested by fitting
29 models with 1, 2, 3 and 4 pulses of abundance. Under the hypothesis that there

30 are incoming pulses of abundance, the best model should have more than one pulse
31 of abundance, while under the alternative hypothesis of no flows from outside the
32 Ecuadorian sub-region, the best model should have just one pulse of abundance,
33 the pulse corresponding to the annual recruitment of squids that grow to the size
34 captured and retained by the fishing gears. We show here that the best model for
35 the Ecuadorian weekly catch, effort and mean weight data is a model with three
36 pulses of abundance, thus supporting the hypothesis in the conceptual proposal of
37 Wiff and Roa-Ureta (2021).

38 **Keywords:** stock assessment; generalized depletion models; flying jumbo squid; South-East
39 Pacific

40 1 Introduction

41 The flying jumbo squid fishery extends over the whole Eastern Pacific Ocean yielding the
42 largest volume of landings of any invertebrate fishery worldwide, reaching over a million
43 tonnes in recent years (Fig. 1). In 2014 Ecuadorian artisanal fleets joined the exploitation
44 of this large stock with significant catches, reaching a maximum in 2018, with over 30
45 thousand tonnes.

46 In 2018, the Instituto Público de Investigación de Acuicultura y Pesca (IPIAP) of
47 Ecuador carried out an extensive sampling program of the catch of the jumbo squid stock
48 by an artisanal fleet using a variety of fishing gears but mainly jigging. This program
49 covered 2162 fishing trips over the whole year, and they accounted for 6% of the total
50 Ecuadorian catch of the jumbo squid that year. In this note I use these catch and fishing
51 effort data from 2018, along with mean weight data taken in separate sampling effort, to
52 fit an intra-annual generalised depletion model (Roa-Ureta, 2012). This idea follows the
53 advice of an international team of experts that reviewed the state of of stock assessment
54 modelling of cephalopod fisheries (Arkhipkin et al., 2021). The model will not evaluate
55 absolute stock abundance because not all the catch and fishing effort are included in the
56 data. Nevertheless, the model will be used to test the hypothesis of the existence of
57 multiple inputs of abundance to the Ecuadorian sub-region.

58 In a separate note (Wiff and Roa-Ureta, 2021) we are proposing a regional stock
59 assessment model based on multi-annual generalised depletion models (Roa-Ureta, 2015;
60 Roa-Ureta et al., 2019) with flows of stock among all sub-regions in the wider South-East
61 Pacific Ocean. Under the proposed region-wide stock assessment model, there are several
62 inputs and outputs of stock abundance due these flows among sub-regions. Therefore,
63 the present note is a proof of concept for the viability of the regional stock assessment
64 proposal in Wiff and Roa-Ureta (2021).

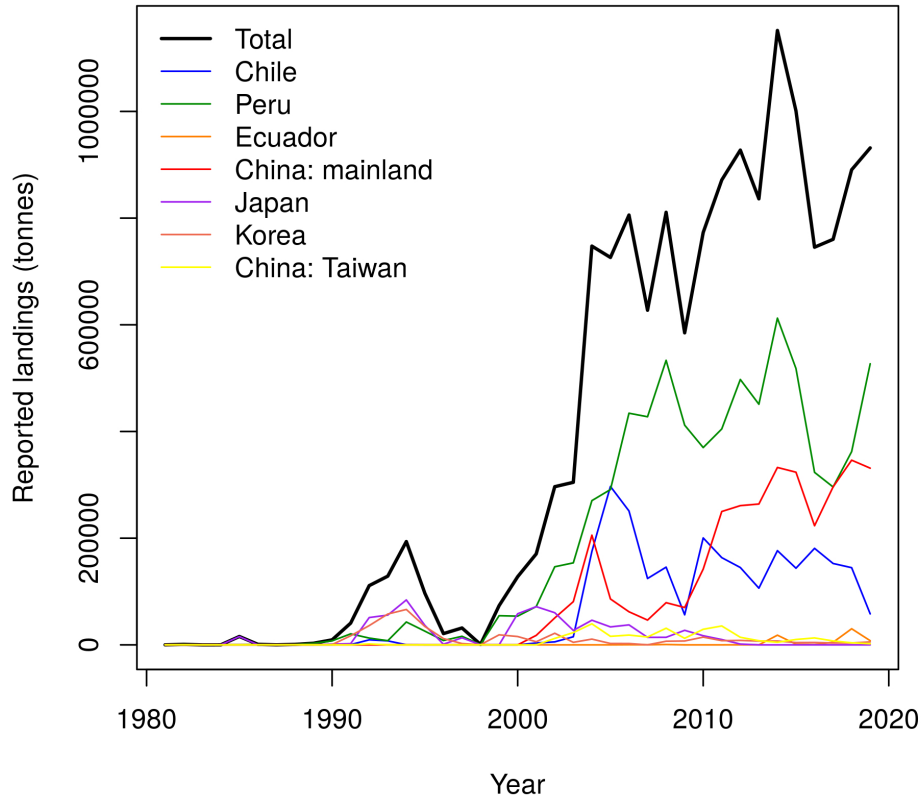


Figure 1: Historical landing records of the flying jumbo squid in FAO database (FAO, 2021) in the South-Eastern Pacific Ocean.

2 Ecuadorian Data

The sampling program conducted by IPIAP in 2018 recorded the catch and several other identification and classification measures per fishing trip with dates of sailing and arrival to port of 2162 fishing trips. No specific measure of fishing effort (such as number of time spent fishing) was recorded. I turned these granular data into a weekly aggregation of catch by all boats sampled during any given week. To match that catch, as a result, with a suitable measure of fishing effort, as one of the causes of the catch, I counted the number of fishing trips per week.

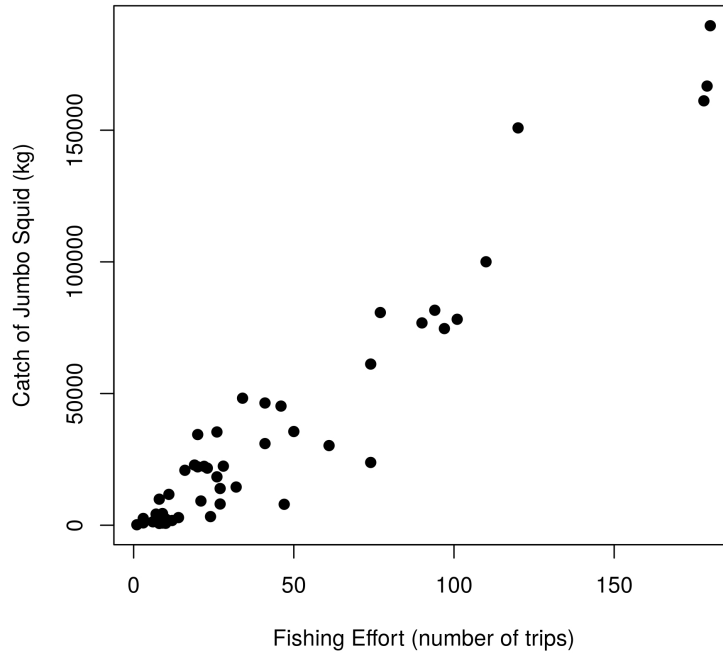


Figure 2: Fishing effort and catch relationship in the sample of fishing trips of the Ecuadorian jumbo squid fishery conducted by IPIAP.

73 Fig. 2 shows the resulting connection between fishing effort and catch. There is a
 74 very strong connection between the chosen measure of fishing effort and the resulting
 75 catch for the sample of fishing trips in IPIAP’s database. This was to be expected given
 76 the large fraction (6%) of the total Ecuadorian catch that was covered by this sample of
 77 fishing trips.

78 An additional database compiled and curated by IPIAP included 6798 individual
 79 squids sampled from the commercial catch during the period 2013 to 2020. This database
 80 contained data on mantle weight with the month of the sample being recorded. I used
 81 R package MMWRweek (Niemi, 2020) to assign week of the year to the monthly mantle
 82 weight data at a randomly selected day within the month. This allowed matching the
 83 fishing effort and catch data with the mean weight data at the cost of introducing some
 84 timing noise. Further random noise was added to this weekly mantle weight data by
 85 sampling from truncated normal distributions using R package Runuran (Leylold and
 86 Hormann, 2020) and the mean mantle weight data and its standard deviation. In this
 87 manner the mantle weight data matched to fishing effort and catch data added sampling
 88 variation in the biological sampling to the model. The resulting mean mantle weight
 89 vector for the model as well as the original data are shown in Fig. 3.

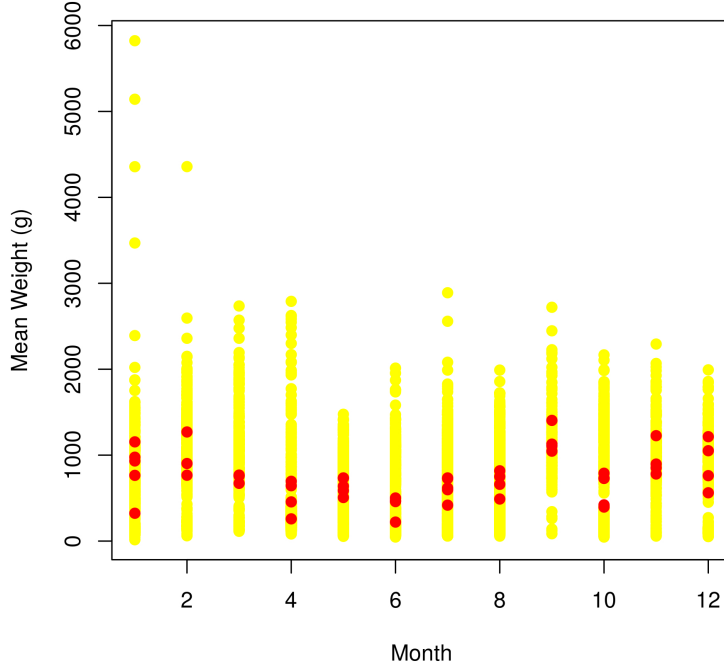


Figure 3: Mean monthly weight of jumbo squid in IPIAP's database (yellow dots) and the re-sampled mean weight per week to use in the model (red dots).

3 Intra-Annual Generalised Depletion Model

Generalised depletion models are depletion models for open populations with nonlinear dynamics. Intra-annual versions work with rapid time step data and are fitted to one season of fishing (Roa-Ureta, 2012; Roa-Ureta et al., 2015, 2021). In this application, the general form of the model is

$$C_t = kE_t^\alpha N_t^\beta$$

$$C_t = kE_t^\alpha e^{M/2} \left(N_0 e^{-Mt} - e^{M/2} \left[\sum_{i=1}^{i=t-1} C_i e^{-M(t-i-1)} \right] + \sum_{j=1}^J I_j P_j e^{-M(t-\tau_j)} \right)^\beta \quad (1)$$

where t is a week of the year, C is the expected catch under the model, k is the scaling, a proportionality constant which is comparable to catchability (although more general, see Roa-Ureta (2012)) having units of $\text{effort}^{-1} \times \text{abundance}^{-1}$, E is the fishing effort E modulated by the effort-response parameter α , N is stock abundance modulated by the abundance-response parameter β , M is the weekly natural mortality rate, N_0 is initial

100 abundance, I_j is an indicator variables taking values of 0 before an exogenous pulse
 101 of abundance enters the vulnerable stock, and 1 afterwards, J is the total number of
 102 abundance pulses, P_j is the magnitude of pulse of abundance j , and tau_j is the week at
 103 which pulse of abundance j happens along the season. I fitted models of this kind with
 104 J taking values of 1, 2, 3 and 4, thus describing hypotheses with different numbers of
 105 in-season exogenous pulses of abundance.

106 The model in Eq. 1, in its four variants ($J = 1, 2, 3, 4$) is the process model, the
 107 postulated mechanism linking the true catch C_t to fishing effort and abundance, which
 108 is assumed to be fairly complete and exact, with negligible process error. The true catch
 109 time series however, is not observed. Instead, a random time series $\chi_{f,t}$ is observed
 110 and its expected value is $C_{f,t}$. Thus the catch time series is a random variable and the
 111 stock assessment model is completed with a statistical model where $\chi_{f,t}$ has a probabil-
 112 ity distribution, a specific parametric distribution. In this proposal, two distributions
 113 were implemented for each fleet, normal and lognormal, corresponding with additive or
 114 multiplicative hypotheses for the observations of catch. In implementing the normal and
 115 lognormal distributions for the fleet's catch data, I fitted models with the exact nor-
 116 mal and exact lognormal distributions and adjusted profile approximations, where the
 117 dispersion parameters are eliminated from the inference. These approximations are as
 118 follows,

$$l_p(\boldsymbol{\theta}; \{\chi_t, E_t\}) = \begin{cases} \frac{T-2}{2} \log \left(\sum_{i=1}^T (\chi_t - C_t)^2 \right) & Normal \\ \frac{T-2}{2} \log \left(\sum_{i=1}^T (\log(\chi_t) - \log(C_t))^2 \right) & Lognormal \end{cases} \quad (2)$$

119 where l_p is the negative log-likelihood function, $\boldsymbol{\theta}$ is the vector of parameters, $\{\chi_t, E_t\}$ are
 120 the catch and effort data, C_t is the predicted catch according to the model in Eq. 1, and
 121 T is the total number of weeks. These negative log-likelihood functions are minimised
 122 numerically as a function of $\boldsymbol{\theta}$ to estimate maximum likelihood parameter values and their
 123 covariance matrix. The free parameters vector is $\boldsymbol{\theta} = (N_0, M, k, \alpha, \beta, \{P\})$. The model
 124 was fit using R package CatDyn (Roa-Ureta, 2018).

125 4 Results

126 None of the intra-annual generalised depletion models with two in-season exogenous in-
 127 puts of abundance yielded successful numerical convergence results. Furthermore, all
 128 model variants fitted to the lognormal distribution (both the exact version and the ad-
 129 justed profile approximation) yielded poor numerical results, with large absolute values
 130 of numerical gradients and/or pathological Hessian matrix, or did not converge at all.
 131 Thus model selection is restricted to variants with 1, 3 or 4 exogenous in-season pulses
 132 of abundance and the exact and adjusted profile approximation to the normal likelihood.

Table 1: Akaike information criterion (AIC) for the selection of the best working model in Eq. 1 in four version, with 1, 3 or 4 in-season exogenous pulses of abundance.

Variant	Likelihood	AIC	Best model
1	A.P. normal	524	1
3	A.P. normal	492	
4	A.P. normal	494	
1	Exact normal	494	1
3	Exact normal	460	
4	Exact normal	462	

Fleet = fibra, Perturbations = 3, Distribution = Apnormal, Numerical algorithm = CG

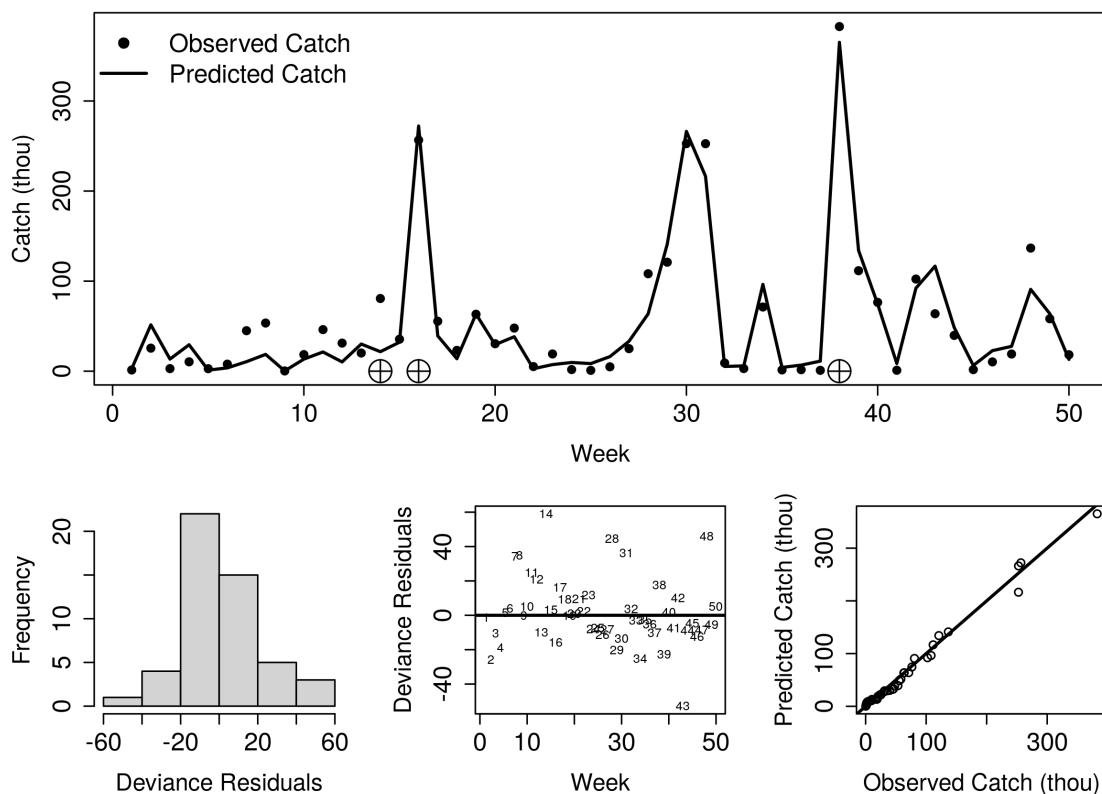


Figure 4: Top panel: fit of the intra-annual generalised depletion model to the catch and fishing effort data of the Ecuadorian sampled fleet during 2018 (target symbols indicate weeks at which the inputs of abundance happened). Bottom left panel: histogram of residuals. Bottom mid panel: cloud of residuals. Bottom right panel: quantile-quantile plot.

133 Under both versions of the normal likelihood, the Akaike Information Criterion identifies the model with three pulses of abundance as the best working model (Table 1).
 134
 135 To select between these two variants, we note that the mean coefficient of variation of

136 parameters estimated under the adjusted profile normal variant was 79.5% while the
 137 same average for the model variant fitted with the exact normal likelihood was 119.5%.
 138 Therefore, on account of better precision of estimates, the 3-inputs of abundance model
 139 fitted with the adjusted profile normal approximation to the likelihood was retained as
 140 the best working model.

141 The fit of this model to the data is shown in Fig. 4. The top panel shows model
 142 predicted catch and observed catch in numbers of squids. Bottom panels are diagnostics
 143 plots to check the quality of the fit from several measures from the distribution of residu-
 144 als. It is noted that in addition to having model predictions that closely follow the data,
 145 diagnostic residual analysis indicate a good fit of the model to the data, with symmetric
 146 residuals histogram, a shapeless cloud of residuals, and very good connection between
 147 quantiles of the observed and predicted random variable.

148 Another useful diagnostics plot is the histogram of correlation coefficients between
 149 parameter estimates. A good model must have those correlation coefficients well-centred
 150 around zero, meaning that all parameters make unique and necessary contributions to the
 151 fit of the data. Although this histogram for the selected model (Fig. 5) is quite broad, it
 152 is concentrated around 0. It could be noted as well that other model variants had worse
 153 or similar histogram of correlations. Thus this additional diagnostic examination further
 154 supports the result that the model with three exogenous in-season pulses of abundance
 155 and the adjusted profile normal distribution for the data is the best working model.

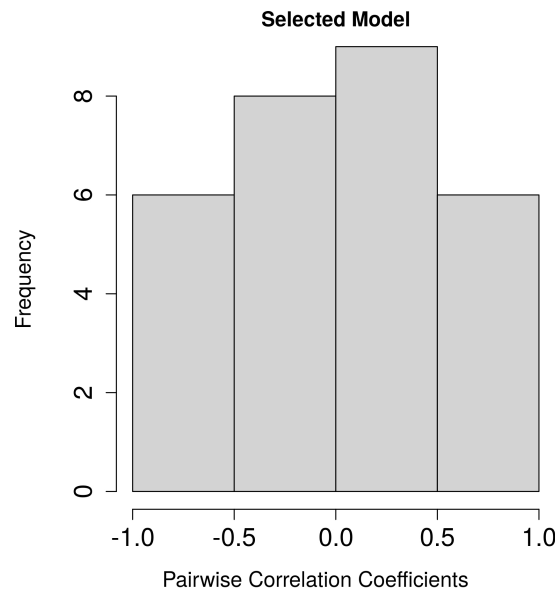


Figure 5: Histogram of correlation coefficients between parameter estimates of the best generalised depletion model for the catch and fishing effort data of the Ecuadorian sampled fleet during 2018.

156 5 Discussion

157 Under the hypothesis that the inputs of jumbo squid abundance to the vulnerable stock
158 during the 2018 season in Ecuadorian waters happen only because of somatic growth, i.e.
159 squids becoming large enough to be vulnerable to the various gears employed to fish them,
160 we would expect a single pulse of abundance in a generalised depletion model. This would
161 be the annual pulse of recruitment to the fishery. This is not what we have obtained.
162 We have found that the best model includes three pulses of abundance. Moreover, two of
163 those pulses of abundance happened in April, and the third one happened in September,
164 which is very far apart along the season. When examining the variation in monthly
165 weight (Fig. 3 we find that in April the mean weight is one of the lowest along the year
166 while in September the opposite is true. Therefore, those two pulses of abundance in
167 April probably are the annual recruitment due to growth while the pulse in September is
168 more likely the result of immigration.

169 6 Conclusions

- 170 • A database of fishing effort and catch at rapid time steps plus mean weight data
171 allows assessment of the jumbo squid fishery in the South-East Pacific with gener-
172 alised depletion models.
- 173 • Intra-annual generalised depletion modelling with Ecuadorian data from one year
174 supports the regional stock assessment model proposal by Wiff and Roa-Ureta
175 (2021) in the sense that it provides evidence in favour of the existence of flows
176 among sub-regions in the wider regional context.
- 177 • Generalised depletion models are appropriate to assess the jumbo squid fishery in
178 the South-East Pacific.

179 References

- 180 Arkhipkin, A.I., Hendrickson, L.C., Payá, I., Pierce, G.J., Roa-Ureta, R.H., Robin, J-P.,
181 Winter, A. 2021. Stock assessment and management of cephalopods: advances and
182 challenges for short-lived fishery resources. *ICES Journal of Marine Science* 78, 714–
183 730.
- 184 Berger, T., Sibeni, F., Calderini, F. 2021. FishStatJ, a tool for fishery statistics analysis,
185 release 4.01.5. FAO, Fisheries Division, Rome.
- 186 Roa-Ureta, R.H. 2012. Modeling In-Season Pulses of Recruitment and Hyperstability-

187 Hyperdepletion in the *Loligo gahi* Fishery of the Falkland Islands with Generalized
188 Depletion Models. ICES Journal of Marine Science 69, 1403–1415.

189 Roa-Ureta, R.H., 2015. Stock assessment of the Spanish mackerel (*Scomberomorus com-*
190 *merson*) in Saudi waters of the Arabian Gulf with generalized depletion models under
191 data-limited conditions. Fisheries Research 171, 68–77.

192 Roa-Ureta, R.H., Molinet, C., Bahamonde, N., Araya, P. 2015. Hierarchical statistical
193 framework to combine generalized depletion models and biomass dynamic models in
194 the stock assessment of the Chilean sea urchin (*Loxechinus albus*) fishery. Fisheries
195 Research 171, 59–67.

196 Roa-Ureta, R.H., Santos, M.N., Leitão, F. 2019. Modelling long-term fisheries data to
197 resolve the attraction versus production dilemma of artificial reefs. Ecological Modelling
198 407, 108727.

199 Roa-Ureta, R.H., Henríquez, J., Molinet, C. 2020. Achieving sustainable exploitation
200 through co-management in three Chilean small-scale fisheries. Fisheries Research 230,
201 105674.

202 Roa-Ureta, R.H., Fernández-Rueda, M.P., Acuña, J.L., Rivera, A., González-Gil, R.,
203 García-Flórez, L. 2021. Estimation of the spawning stock and recruitment relationship
204 of *Octopus vulgaris* in Asturias (Bay of Biscay) with generalized depletion models:
205 implications for the applicability of MSY. ICES Journal of Marine Science. pdf.

206 Wiff, R., Roa-Ureta, R.H. 2021. Regional stock assessment of the flying jumbo squid in
207 the South-Eastern Pacific: a conceptual proposal. Presented to OROP-PS, October
208 2021.

209 Niemi, J. 2020. MMWRweek: Convert Dates to MMWR Day, Week, and Year. R package
210 version 0.1.3. <https://CRAN.R-project.org/package=MMWRweek>

211 Leylold, J., Hormann, W. 2020. MWRweek: Convert Dates to MMWR Day, Week, and
212 Year. R package version 0.1.3. <https://CRAN.R-project.org/package=MMWRweek>

213 Roa-Ureta, R.H. 2018. Fishery stock assessment by catch dynamics models, CatDyn
214 version 1.1-1. <https://CRAN.R-project.org/package=CatDyn>